



Alkaline activation synthesis by graphite/calcite mortar and the effect of experimental conditions on compressive strength

Nurşah Küçük¹ · Sevil Çetinkaya Gürer¹

Received: 27 August 2022 / Revised: 5 June 2023 / Accepted: 14 June 2023 / Published online: 20 July 2023
© The Author(s) under exclusive licence to Australian Ceramic Society 2023

Abstract

The construction industry is an application area that has continuity all over the world and requires cheap, durable, and environmentally friendly materials. Synthesis with alkali activation includes materials that have come to the fore in the construction industry in recent years. In this study using alkali activation method, a graphite/calcite mortar was prepared by optimizing the experimental conditions and its properties were investigated. The effects of $\text{Na}_2\text{SiO}_3/\text{NaOH}$ mass ratio, NaOH solution concentration, and graphite content variables on structure and compressive strength in alkaline activation synthesis were investigated. It was determined that the samples reached a compressive strength of 21 MPa at the end of 28 days when the $\text{Na}_2\text{SiO}_3/\text{NaOH}$ ratio was 2 and the NaOH concentration was 10 M. In the continuation of the optimized experimental conditions, the effect of the amount of graphite on the compressive strength was examined between 5 and 100% (w/w). Structural properties of the samples were investigated by X-ray diffraction and Fourier transform infrared spectroscopy, and their morphological properties were investigated by scanning electron microscopy. It was determined that C–S–H gel was formed and samples with heterogeneous morphology were synthesized.

Keywords Calcite · Graphite · Alkaline activation · Compressive strength

Introduction

Alkaline active materials, generally known as geopolymers, are of great interest to researchers [1]. Especially in recent years, these materials have come to the fore among building materials due to their unique properties such as high strength, superior chemical resistance, and thermal stability [2]. In addition, one of the most important properties of alkali active materials is their environmental friendliness. The reason for this is that it does not need a process at high temperatures. In the production of Portland cement, CO_2 emissions occur with clinker formation and kiln firing. Since this process is not required in activation, CO_2 emission is low [3]. It has been reported in research that materials prepared with alkaline activity do not cause serious harm to the environment due to their low carbon footprint [4]. For example, it has been reported that slag-based materials synthesized by alkaline

activation cause approximately 25–50% less CO_2 emissions compared to Portland cement [5].

It is possible to classify materials synthesized by alkaline activation as materials with low or high Ca content. Systems with low Ca can be called geopolymers. Its main products in alkaline environment are N–A–S–H gel and three-dimensional SiO_4 and AlO_4 structures. In systems containing high calcium, C–(A)–S–H gel is formed in alkaline environment. This is the case in systems where these two gels appear together [2]. As a result, gel products and units formed during the synthesis of geopolymers and alkali-activated materials are different [6]. Geopolymers formed by the reaction of alumina silicates in an alkaline medium are environmentally friendly, are cheap, have low density, have high heat resistance, have low CO_2 emission, and are simply processing materials [7–9]. This process, called the alkaline activation method, involves mixing alumina silicates with an activator solution in an alkaline medium [10]. NaOH and Na_2SiO_3 solution are among the most used alkalis [11]. Geopolymer materials are synthesized with various raw materials such as fly ash, volcanic ash, pumice, kaolin, metakaolin, granulated blast furnace slag, and wastes [8, 12–16]. During the geopolymer

✉ Nurşah Küçük
nkutuk@cumhuriyet.edu.tr

¹ Faculty of Engineering, Chemical Engineering Department, Sivas Cumhuriyet University, Sivas 58140, Turkey

synthesis, parameters such as the composition of the raw material, alkali concentration, and curing temperature are important. Because it affects the structure and properties of the final product to be obtained at the end of the process [17]. Considered a new generation cement, geopolymers (alkali activated binders) are among the most important building materials in the world [18].

In recent years, carbon-based materials such as graphite, carbon fiber, and multi-walled carbon nanotubes (MCNTs) have been preferred in the cement sector due to their properties. For example, carbon fiber has very good mechanical properties, and unmatched electrical and thermal conductivity, while MCNT has a high strength and modulus of elasticity. These materials are actually different forms of graphite structure [19]. Graphite is a common material that can be used in different areas (e.g., lubricity, thermal shock resistance) with important physical and chemical properties such as high thermal conductivity, low coefficient of thermal expansion, and resistance to solvent corrosion [20]. It is formed by non-covalent π - π bond interaction of graphene sheets [21]. Calcite is an inexpensive mineral material abundant in nature as the most stable polymorph of calcium carbonate (CaCO_3) [22, 23]. Calcite, which is usually found in pure form, may contain impurities such as magnesium, iron, and manganese [24]. Studies have shown that the use of Ca salts accelerates the setting time by forming heterogeneous nucleation centers in the samples [25]. In some studies in the literature, metakaolin, which is one of the most used materials in the synthesis of geopolymers, has been used by modifying graphite. In the study of Zhang et al., a geopolymer was synthesized with potassium silicate using metakaolin and graphite. When the effect of the amount of graphite in the geopolymer was examined, it was reported that when added in an appropriate amount, it had a positive effect on the flexural strength and dielectric constant of the samples [7]. In a study in which calcite was added to the metakaolin geopolymer, it was determined that while the amount of calcite was 6% by weight, the compressive strength of the geopolymer reached 28.88 MP [26].

In this study, graphite/calcite mortar was prepared and the compressive strengths of the samples were examined at the end of the 28th day. The effects of $\text{Na}_2\text{SiO}_3/\text{NaOH}$ mass ratio and NaOH concentration parameters on the compressive strength and material structure on the alkaline activation process were investigated. Structural properties of the samples were analyzed by XRD and FTIR characterization analysis, and morphological properties were analyzed by SEM technique. For the prepared graphite/calcite mortar, the amount of calcite and graphite was changed as a percentage and its effect on the compressive strength was examined. In this study, the effect on the structure and compressive

strength was investigated by using materials containing C and Ca instead of materials containing Si and Al. The contributions of this study are several folds:

- As far as we know, the synthesis of mortar with alkali activation with the use of graphite and calcite raw materials was studied by us for the first time.
- The process was optimized by examining the parameters affecting the compressive strength and structure of the graphite/calcite mortar.

Material and method

Materials

The raw materials to be used in the study were chosen as calcite and graphite. The calcite used in the study was obtained from the Betta Gypsum and Construction Chemicals factory and from the graphite Nanografi Company. The density of sodium silicate used in the experiments was 1.4 g/cm^3 and obtained from Orbital Chemical Company. Table 1 shows the chemicals used in process and their properties.

Experimental method

The graphite used as the starting material was first mixed with NaOH solution for 5 min. Then, the mixing process was continued by adding calcite. The alkali activation process was continued with the addition of water and Na_2SiO_3 as needed. The mixing process was continued for 20–25 min until the mortar became homogeneous. Then, the resulting mortar was poured into steel and cubic molds measuring $40 \times 40 \times 40 \text{ mm}^3$. After the molding process, the mortar was left to rest for 24 h. It was observed that the drying of the samples prepared with high NaOH concentration (e.g., 20 M) was delayed after molding and they were left to rest for up to 48 h. Cubic specimens, which were removed from the mold the next day, were cured in an oven at $65 \text{ }^\circ\text{C}$ for 5 days. The curing process was continued by treating the material in the oven at $40 \text{ }^\circ\text{C}$ for 2 h and then at $65 \text{ }^\circ\text{C}$. Samples prepared after

Table 1 Properties of raw materials used in synthesis

Raw materials	Chemical formula	Purity (%)	Molecule weight (g/mol)
Graphite	C	99	12
Calcite	CaCO_3	95	100
Sodium hydroxide	NaOH	99	40
Sodium silicate	Na_2SiO_3	99	122

curing were allowed to rest at room temperature for up to 28 days. In the synthesis, the NaOH aqueous solution was prepared as M (mol/L), and the Na₂SiO₃ solution was used undiluted. The experimental flow chart of the alkali activation process is given in Fig. 1.

Characterization

Attenuated total reflection-fourier transform infrared spectroscopy analyses of the synthesized samples were performed with Perkin Elmer Spectrum 400 model in the range of 4000–400 cm⁻¹. XRD analyses of the samples were performed on Bruker AXS D8 Advance Model XRD device operating at 40 mA, 40 kV values at a scanning speed of 0.020°/min (CuKα = 1.541871°) in the range of 2θ = 5°–90°. Its morphological structure was investigated with SEM (Leo 440 Computer Controlled Digital). In the study, the compressive strength analyses of the samples were made with the Utest Material Testing Equipment (Novo technik) brand device given in Fig. 1.

Results and discussion

Effect of Na₂SiO₃ mass ratio

Various alkali activators such as sodium silicate, sodium hydroxide, sodium carbonate, and potassium hydroxide can be used in alkali activation synthesis [27]. Literature studies show that Na₂SiO₃/NaOH mass ratio and NaOH concentration are process parameters that significantly affect the compressive strength [28]. Possible reactions of graphite/calcite mortar are given in Eqs. 1, 2, and 3 [1, 29]. In reactions with high alkalinity, the calcium carbonate reaction can give the necessary Ca²⁺ ions for the formation of the C–S–H gel. The precipitated C–S–H gel may causes an increase in compressive strength [30].

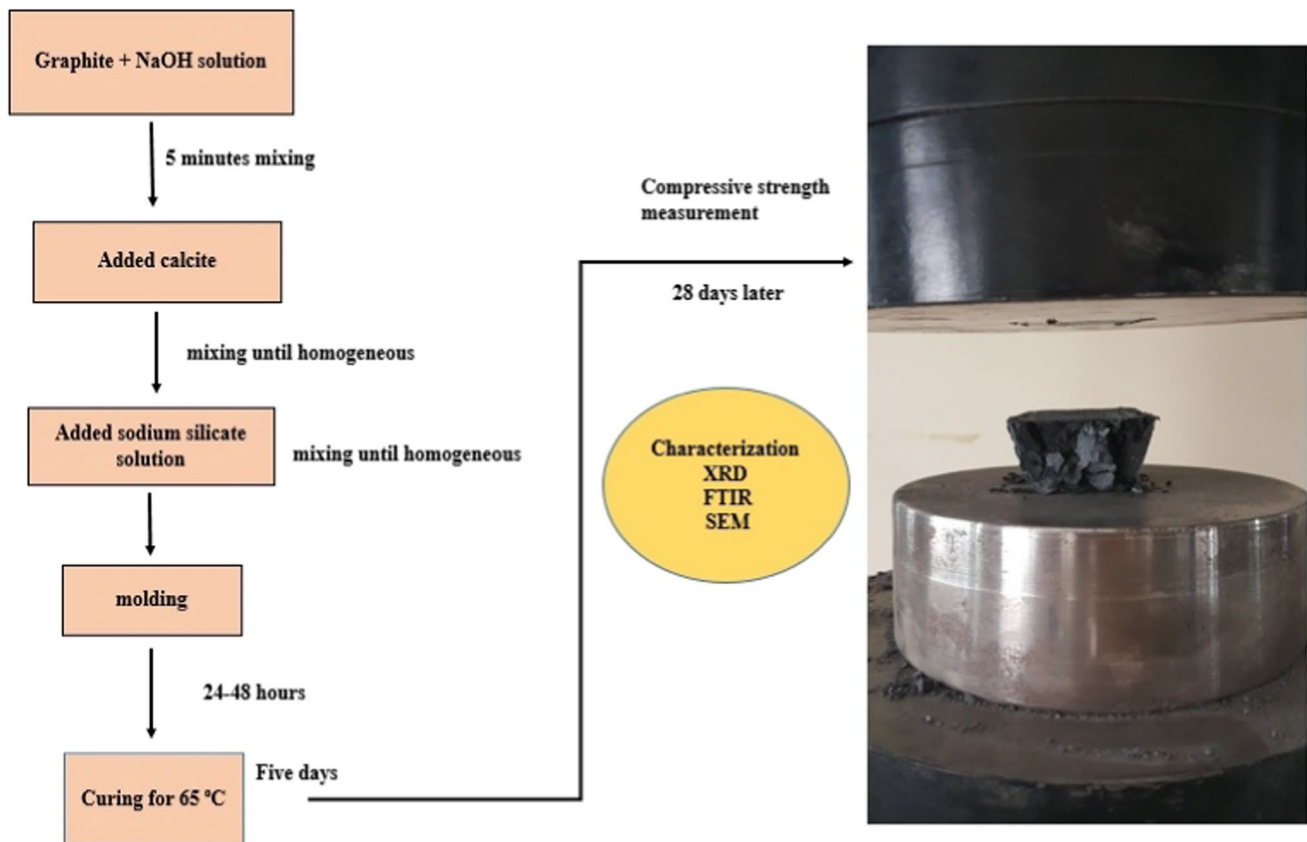
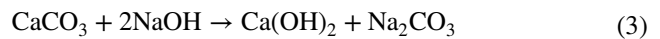
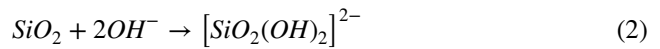


Fig. 1 Schematic images of alkali activation process

The effects of $\text{Na}_2\text{SiO}_3/\text{NaOH}$ mass ratio, NaOH concentration, and graphite amount were investigated while preparing the samples. XRD spectra of calcite and graphite are given in Fig. 2 a and b. The sharp peak at $2\theta = 29.4^\circ$ in Fig. 2 a is a characteristic peak attributed to the crystal structure of calcite. Similarly, the peaks at 23.06° , 39.46° , 43.2° , and 47.5° are characteristic peaks of calcite [30, 31]. The sharp peak seen at $2\theta = 26.4^\circ$ in Fig. 2 b is the characteristic peak pointing to the hexagonal and crystalline structure of graphite [32–34].

In Fig. 3, there are XRD spectra of samples prepared in the presence of different $\text{Na}_2\text{SiO}_3/\text{NaOH}$ mass ratios and 10 M NaOH solution and 5% graphite and 95% calcite. The

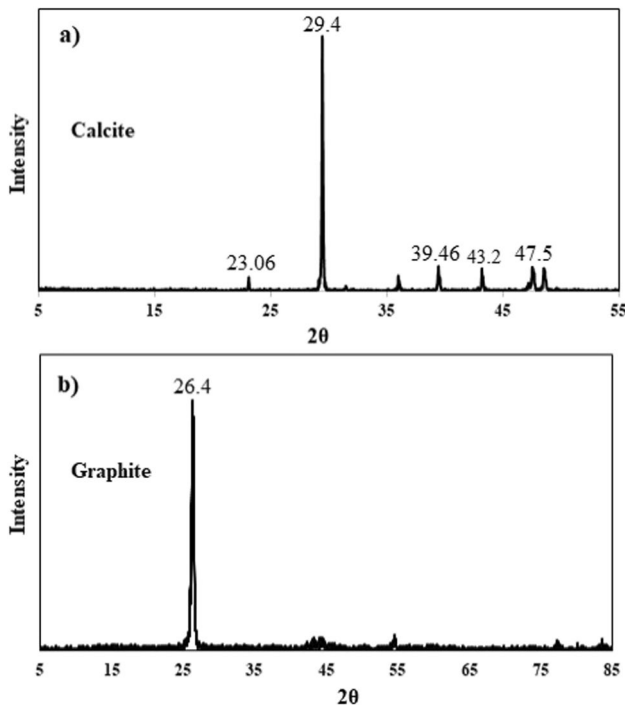
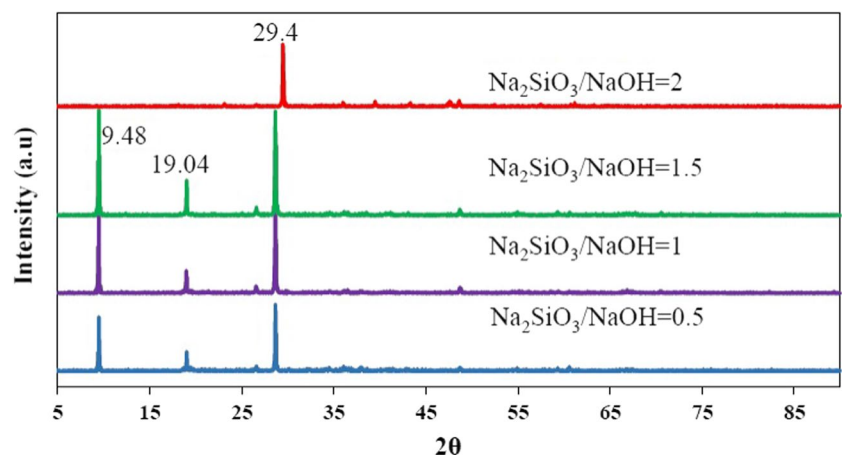


Fig. 2 XRD patterns of a calcite and b graphite

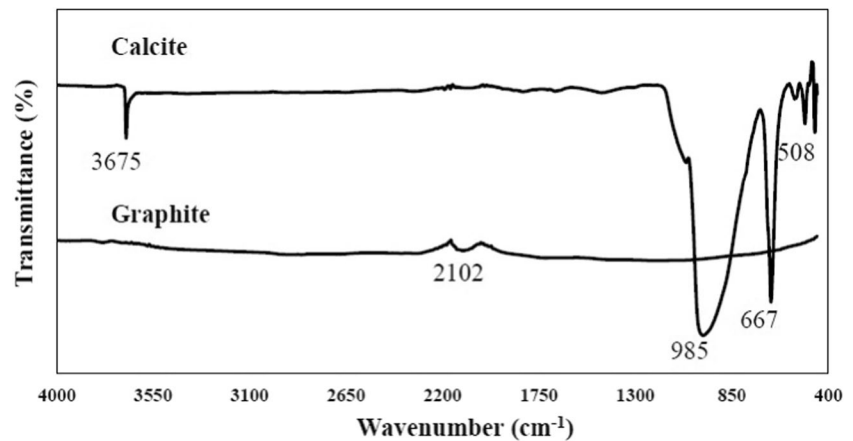
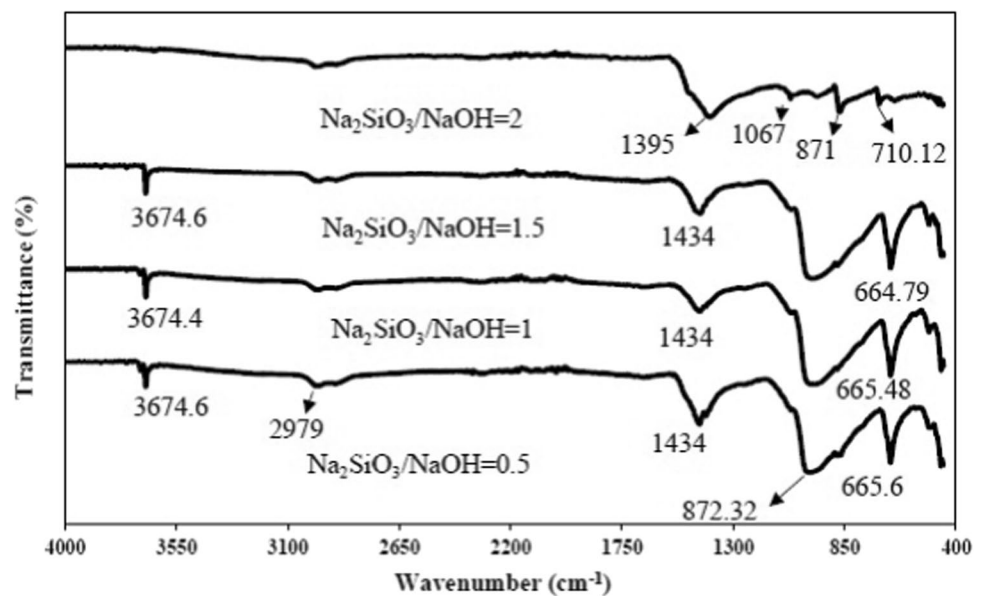
Fig. 3 XRD patterns for samples with different $\text{Na}_2\text{SiO}_3/\text{NaOH}$ mass ratio



results show that in all the synthesized samples, the characteristic peak of calcite appeared at $2\theta = 29.4^\circ$. The reason for this situation may be both the amount of calcite being higher than the amount of graphite and the insoluble calcite molecules in alkaline environment [22]. It has been reported that unreacted raw materials have a negative effect on the compressive strength [35]. Erfanimanesh et al. reported that this peak at 29.4° indicates the presence of a C–S–H (calcium silicate hydrate) gel or calcite [18]. In the samples, new peaks appeared at 9.48° and 19.04° . New peaks appearing around $2\theta = 19.04^\circ$ may be attributed to $\text{Ca}(\text{OH})_2$ formation [36]. This result shows that calcite is activated with NaOH according to Eq. 3 and $\text{Ca}(\text{OH})_2$ is formed. The lack of this peak in the sample with a $\text{Na}_2\text{SiO}_3/\text{NaOH}$ mass ratio of 2 denotes the absence of $\text{Ca}(\text{OH})_2$ formation.

FTIR spectra of calcite and graphite are given in Fig. 4. There is only one peak occurring at 2102 cm^{-1} in the graphite spectrum and may be due to the presence of atmospheric CO_2 [36]. In the calcite spectrum, there are peaks representing the carbonate structure. The peak CO_3^{2-} seen at 667 cm^{-1} of calcite is attributed to in-plane bending, while the peak CO_3^{2-} seen at 985 cm^{-1} is attributed to symmetrical stretching [37, 38].

In Fig. 5, FTIR spectra of samples prepared according to different $\text{Na}_2\text{SiO}_3/\text{NaOH}$ mass ratios (0.5, 1, 1.5, and 2) are given. The IR peaks observed in the samples and the chemical groups they express are given in Table 2. Peaks appearing at 3674 cm^{-1} in samples prepared in $\text{Na}_2\text{SiO}_3/\text{NaOH}$ mass ratio 0.5, 1, and 1.5 represent O–H asymmetric stretch vibrations. This result shows that free water is converted to bound water during synthesis [39]. In addition, the peak at 3674 cm^{-1} may indicate $\text{Ca}(\text{OH})_2$ formation. This peak disappeared when the $\text{Na}_2\text{SiO}_3/\text{NaOH}$ ratio was 2 [41]. According to the literature, the peak appearing at 2979 cm^{-1} may be related to the C–S–H structure [42]. The peaks at $1395\text{--}1434\text{ cm}^{-1}$ appearing in all samples can be attributed to O–C–O stretching vibration due to sodium carbonate formation [35]. The presence of carbonate may

Fig. 4 FTIR spectrums of calcite and graphite**Fig. 5** FTIR spectrums for samples with different $\text{Na}_2\text{SiO}_3/\text{NaOH}$ mass ratio**Table 2** Infrared spectrum [1, 35, 39, 40]

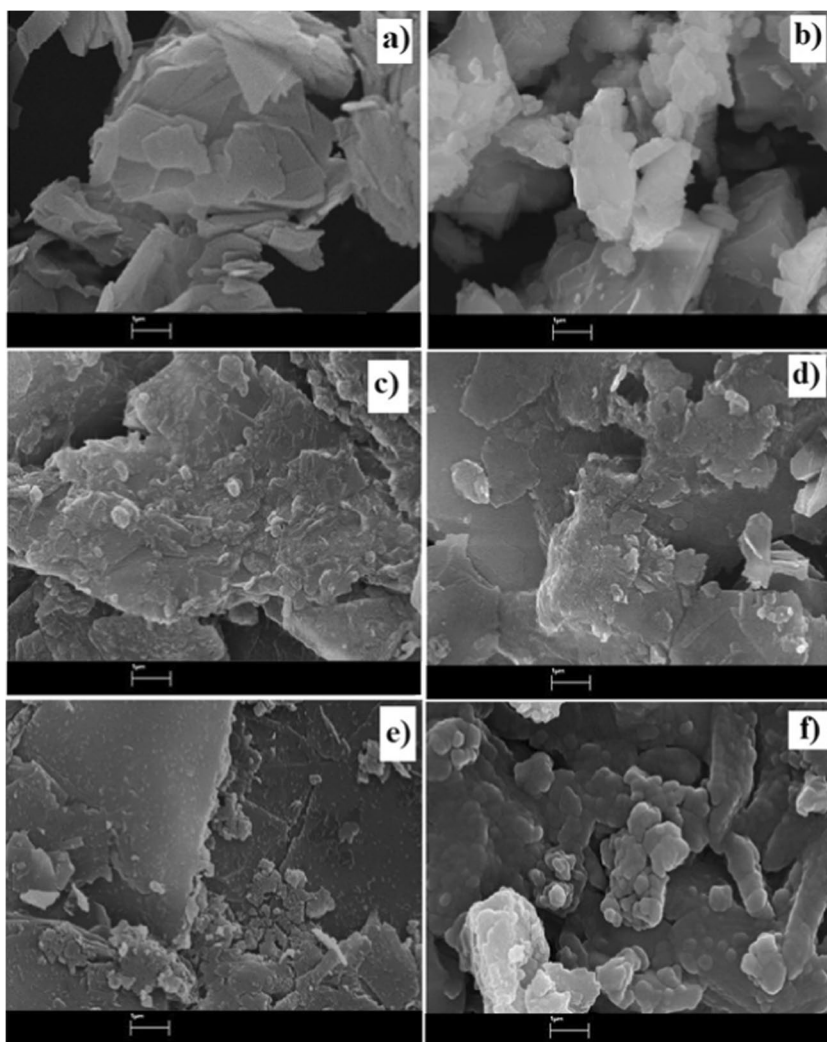
Bond	Wavelength (cm^{-1})
O–H asymmetric stretch vibration	3674
O–C–O stretching vibration	1434
Si–O asymmetric stretching	1067
Si–Al–O bonding	710–664

have arisen from the reaction of free Na^+ ions with atmospheric CO_2 [43]. While the mass ratio of $\text{Na}_2\text{SiO}_3/\text{NaOH}$ is 2, when the spectrum of the synthesized sample is examined, the peak occurring at 1067 cm^{-1} is attributed to the Si–O asymmetric stretch and comes from the C–S–H structure [1, 42]. This peak comes from the Na_2SiO_3 structure and shows that it is formed in the silicate network structure [1, 39]. In addition, no peak was observed at 1067 cm^{-1} in samples with a $\text{Na}_2\text{SiO}_3/\text{NaOH}$ ratio of 0.5, 1, and 1.5. The peaks

appearing at 664, 665, and 710 cm^{-1} in the samples are attributed to Al(IV)–O–Si vibrations. This result shows the formation of the aluminosilicate network [39]. Similarly, the peak occurring at about 871 cm^{-1} in all samples indicates the Si–O stretching vibration from sodium silicate [1]. Some peaks attributed to the calcite structure were also found in the FTIR spectrum of the synthesized samples. The peak at 667 cm^{-1} in calcite and the peak at 665 cm^{-1} in the synthesized samples may have overlapped. In addition, when the $\text{Na}_2\text{SiO}_3/\text{NaOH}$ ratio was 2, the intensity of this peak decreased and shifted to 710 cm^{-1} . This result may indicate that as the amount of Na_2SiO_3 increases, calcite dissolves better and silicate network is established.

The SEM images of the samples prepared with graphite and calcite, and the raw materials used in the synthesis of the sample, and at different $\text{Na}_2\text{SiO}_3/\text{NaOH}$ ratios are given in Fig. 6. When the SEM image (Fig. 6a) of graphite is examined, the clustered particles and layered structure attract

Fig. 6 SEM images **a** graphite and **b** calcite; samples different $\text{Na}_2\text{SiO}_3/\text{NaOH}$ mass ratios **c** 0.5, **d** 1, **e** 1.5, and **f** 2 (all samples at 30000 magnifications and at 1- μm scale)

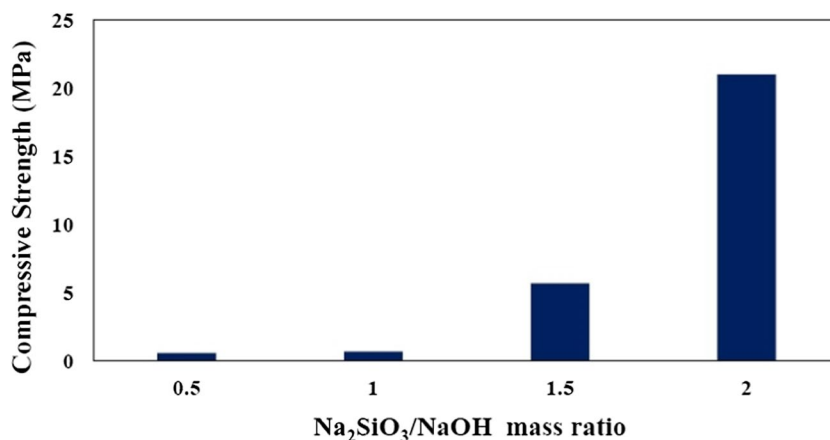


attention [33, 44]. In Fig. 6 b, it is seen that the SEM image of calcite resembles a structure with different geometries, however, including cubic, hexagonal, and crystalline calcite forms [24, 45].

It can be said that the graphite/calcite mortar samples generally have a heterogeneous structure. According to XRD results, there is unreacted calcite. If the amount of Na_2SiO_3 is insufficient during activation, the raw materials may remain unreacted. As the ratio of $\text{Na}_2\text{SiO}_3/\text{NaOH}$ increases, the integrity and compactness of the structure increase [46]. In Fig. 6 c, d, and e, it can be said that the heterogeneity in the structure decreases with the increase in the amount of Na_2SiO_3 in line with the literature. This is because the raw materials dissolve better [47]. Figure 6 f is the sample with the highest amount of Na_2SiO_3 . The sample surface's absence of cracks suggests that the free water has fully reacted [43]. As a result, it is clearly observed that as the $\text{Na}_2\text{SiO}_3/\text{NaOH}$ mass ratio increases, calcite and graphite dissolve better and gelation develops. In Fig. 6 f, it is seen that gelling is more.

It is clearly seen in the Fig. 7 that the compressive strength of the samples increases as the mass ratio of $\text{Na}_2\text{SiO}_3/\text{NaOH}$ increases. The highest compressive strength (21 MPa) was found in the sample with a mass ratio of 2. The reason for this situation may be the increase in compressive strength due to Si^{+3} and Al^{+4} ions released from aluminosilicates [48]. When Na_2SiO_3 increases, the amount of silica gel also increases and polymerization may develop to form a product with high compressive strength [28]. In addition, the formation of $\text{Ca}(\text{OH})_2$ in the sample can cause cracks on the sample surface and reduce its workability [35]. FTIR and XRD data support the formation of $\text{Ca}(\text{OH})_2$ when the $\text{Na}_2\text{SiO}_3/\text{NaOH}$ mass ratio is 0.5, 1, and 1.5. This result may explain the reason for the increase in compressive strength when the $\text{Na}_2\text{SiO}_3/\text{NaOH}$ mass ratio is 2. In Tippayasam et al., $\text{Ca}(\text{OH})_2$ was used as raw material in their studies. The increase in the amount of $\text{Ca}(\text{OH})_2$ in the synthesized geopolymer samples improved the hydration reaction and the formation of C–S–H gel increased. This result also led to an improvement in compressive strength [49]. In our study,

Fig. 7 Compressive strength of samples prepared with different $\text{Na}_2\text{SiO}_3/\text{NaOH}$ ratio (for 28 days)



$\text{Ca}(\text{OH})_2$ formation was observed as a result of the reaction. As the ratio of $\text{Na}_2\text{SiO}_3/\text{NaOH}$ increased, the amount of $\text{Ca}(\text{OH})_2$ formed and therefore the compressive strength may have increased. However, when the $\text{Na}_2\text{SiO}_3/\text{NaOH}$ ratio was 2, the compressive strength reached its highest value and analysis results referring to $\text{Ca}(\text{OH})_2$ formation were not found. The reason for this may be the absence of $\text{Ca}(\text{OH})_2$, which can cause cracks in the structure, and the improved compressive strength. Experiments were continued with this ratio and the effect of NaOH concentration was investigated.

Effect of NaOH concentration

To investigate the effect of alkali activator on graphite/calcite mortar properties, 5, 10, 15, and 20 M concentrations of NaOH solutions were used. When the XRD spectra are examined (Fig. 8), it is seen that the peak seen at $2\theta = 29.4^\circ$ appeared in all samples. This peak comes from calcite and reveals its crystal structure [31]. The reason

why this peak is sharp in all spectra may be the presence of still insoluble calcite [22]. Because calcite has poor solubility in basic media [50]. It is confirmed that calcite is partially soluble in alkaline medium [50, 51]. The increase in NaOH concentration may not have affected the solubility of calcite for this reason. Since the amount of calcite is higher than graphite, it is thought to be the prominent material in the structure.

In Fig. 9, the effect of NaOH concentration on the compressive strength was examined in the range of 5–20 M and the highest compressive strength value was obtained as 21 MPa. While the NaOH concentration was 10 and 20 M, the compressive strength of the samples reached 21 MPa. Increasing the NaOH concentration caused the sample to be much more sticky. Therefore, the workability of the samples decreased. Increasing the NaOH concentration may be unnecessary, as the same compressive strength is achieved at 10 M. Therefore, the optimum NaOH concentration was determined as 10 M.

Fig. 8 XRD pattern of samples prepared with different NaOH concentration

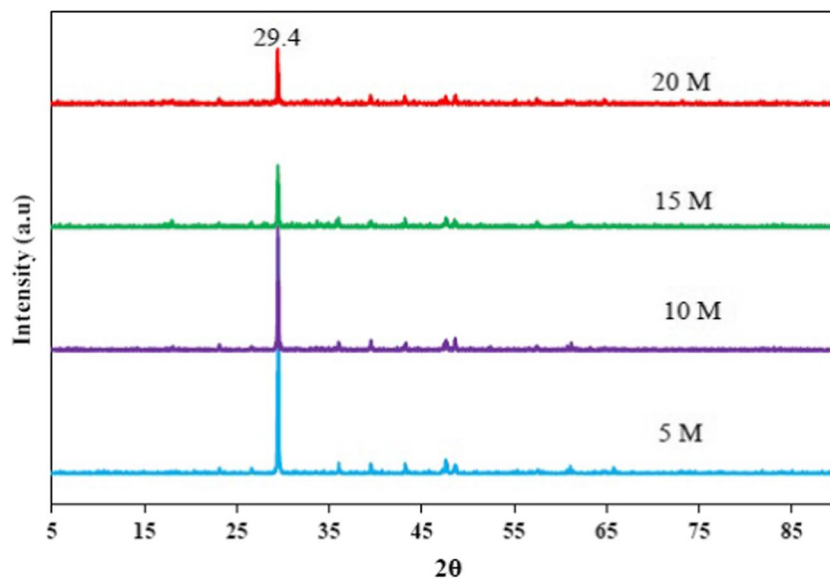
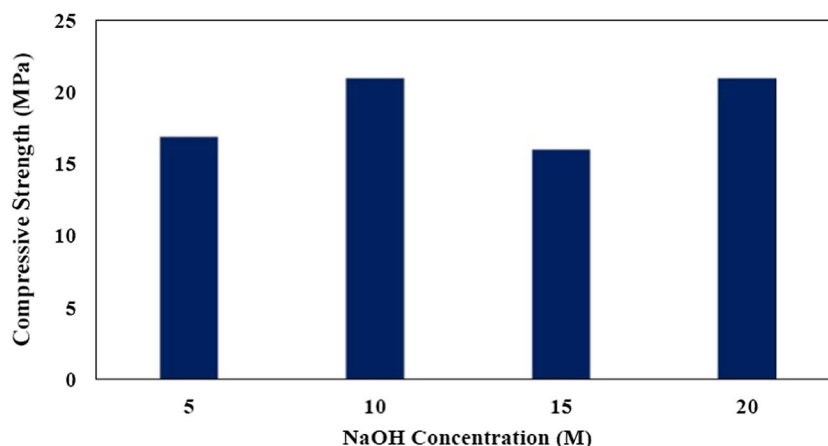


Fig. 9 Compressive strength of samples prepared with different NaOH concentrations (for 28 days)



The literature shows that as the NaOH concentration increases, the compressive strength also increases. This may be due to poor chemical reaction ability at low concentrations [52]. However, when the concentration of NaOH solution increases, the amount of Na^+ ion increases proportionally. In this case, the amount of water is low and the amount of ions is high. Ion transport becomes more difficult and it may reduce the compressive strength [53]. In the other case, similarly, with increasing NaOH concentration, the amount of OH^- ions increases, and accordingly, dissolution and hydrolysis also increase. The appropriate value for compressive strength is reached when the Si and Al load balance is achieved in the tetrahedral structure provided by NaOH [54]. These results may be the cause of the imbalance between the increase and decrease in compressive strength with increasing NaOH concentration.

Effect of graphite amount on compressive strength of graphite/calcite mortar

In the last part of this study, experimental parameters $\text{Na}_2\text{SiO}_3/\text{NaOH}$ mass ratio and NaOH solution concentration were used as optimized in relation to the compressive strength. The effect on the compressive strength was investigated by changing different graphite and calcite percentages on the total solid raw material amount. The compressive strength of the samples at the end of the 28th day was examined by changing the graphite amount (w/w) between 5 and 100%.

In the literature, there are studies on composites synthesized by modifying calcite and graphite with different raw materials. The gel and chemical structures formed in geopolymer and alkali active mortars differ. However, the method used is almost the same. In a study using calcite and fly ash in the literature, it was observed that the compressive strength increased as the amount of calcite increased [55]. In the study of Mizerova et al., it was observed that the compressive strength decreased when

graphite was added to the fly ash geopolymer at different rates. When 2% graphite was added to the fly ash geopolymer, a compressive strength of 17.7 MPa was reached [56]. Calcite and graphite are prepared together and the effect of graphite amount on compressive strength is the last part of this study. The results are given in Table 3. Calcite has low solubility in the presence of alkaline medium. However, the slow solubility of calcite can make it available as a texture material on the surface. In the study of Yip et al., geopolymer was synthesized with calcite and metakaolin. They concluded that calcite can remain on the surface and increase the compressive strength of the gel. It has been reported that the presence of calcite in the geopolymer contributes to the formation of the geopolymer gel. C–S–H

Table 3 Experimental parameters and compressive strengths of the samples synthesized in the study

Graphite percentage (%)	NaOH concentration (M)	$\text{Na}_2\text{SiO}_3/\text{NaOH}$	Compressive strength (MPa)
5	10	0.5	0.6
5	10	1	0.7
5	10	1.5	5.7
5	10	2	21
5	5	2	16.9
5	15	2	16
5	20	2	21
10	10	2	2.5
20	10	2	3.1
30	10	2	1.5
40	10	2	1.8
50	10	2	1.7
60	10	2	3.1
70	10	2	2.3
80	10	2	4.8
90	10	2	3.6
100	10	2	3.5

gel may have developed in our study by providing alkaline activation of calcite and graphite [22]. While the graphite amount was at its lowest value (5%), the compressive strength reached its highest value (21 MPa). The reason for this situation may be that graphite causes agglomeration in the structure, causing defects and heterogeneity in the microstructure [7]. Graphite is a soft and layered material. The bonds between the layers are long and weak. Therefore, its layers are more susceptible to slip and breakage. Due to this property, there are studies in which graphite is used as a filler for composite synthesis [57]. Therefore, the weak mechanical strength of the graphite crystals may cause a decrease in the compressive strength of the samples [58]. In our study, it was observed that the addition of 5% graphite to the composite strengthened the structure in accordance with the literature (Fig. 10) [56].

In Table 4, the compressive strength results of the geopolymer and alkali active cement samples synthesized using different raw materials at the end of the 28th day are given by comparing them. As presented, the raw materials commonly used in geopolymer production are fly ash and kaolin. Calcite and graphite materials are inexpensive materials that are abundantly available. However, graphite has been used little in alkaline activation. It can be used as an important building material for the future with appropriate compressive strength results as a result of the optimization of the alkali activation process. The amount of raw material, alkali concentration, or synthesis method used by each scientist in the preparation of samples may differ. For this reason, the compressive strength of samples prepared with the same raw material is different from each other. In the study of Arioiz et al., the compressive strength reached in the sample prepared with low concentrations of NaOH and fly ash is lower than the sample prepared with fly ash in the study of Ng et al. [54, 59]. This information shows us that many different raw materials can be used in the production of alkali active sample. Achieving optimum compressive strength may vary depending on experimental

Table 4 Twenty-eight-day compressive strength of composites prepared with different raw materials in the literature

Raw materials	Compressive strength (MPa)	References
Fly ash	35	[54]
Metakaolin/calcium carbonate	26	[50]
Kaolinite/calcite	12.68	[13]
PEG added metakaolin	23.9	[60]
Fly ash	11.06	[59]
Limestone/calcite	48.8	[61]
Graphite/calcite	21	This study

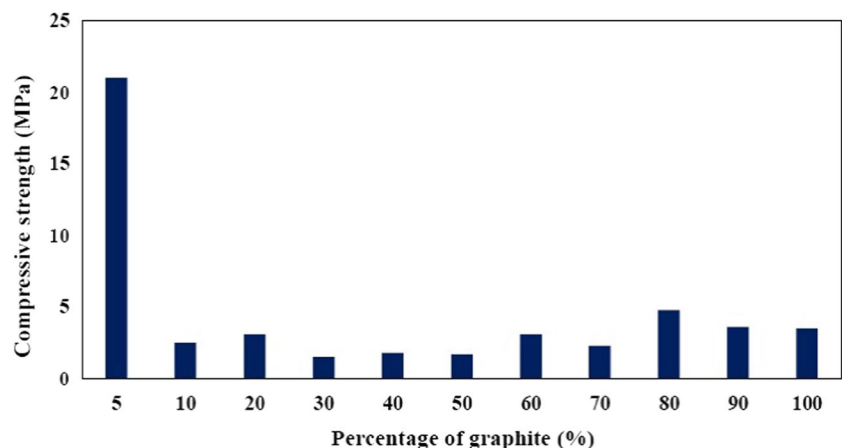
conditions. Calcite and graphite, selected as raw materials in our study, reached a good strength (21 MPa) as a result of alkali activation synthesis.

Conclusion

Alkali active mortar attract attention as promising materials for the rapidly polluted world in recent years due to their environmental friendliness and high compressive strength compared to Portland cement. In this study, the graphite/calcite alkali active mortar was successfully synthesized by optimizing the experimental parameters. According to the results of our research:

1. optimum experimental conditions to prepare graphite/calcite alkali active mortar with the highest compressive strength (21 MPa) were founded as the graphite content of 5%, the concentration NaOH of 10 M, and the ratio of $\text{Na}_2\text{SiO}_3/\text{NaOH}$ of 2;
2. according to the XRD and FTIR results, the solubility of graphite and calcite increased with the increase of the amount of $\text{Na}_2\text{SiO}_3/\text{NaOH}$. In particular, it was observed in the FTIR results that the C–S–H gel and Al(IV)–O–Si

Fig. 10 Effect of graphite amount on compressive strength



bond appeared, from which the silicate network developed. Similarly, $\text{Ca}(\text{OH})_2$ formation was not observed in the sample when the $\text{Na}_2\text{SiO}_3/\text{NaOH}$ mass ratio was 2. This result may be one of the reasons why the compressive strength increases with the increase of the $\text{Na}_2\text{SiO}_3/\text{NaOH}$ mass ratio;

3. it was revealed in the SEM images that the obtained samples were heterogeneous. XRD, FTIR, and SEM analysis results support each other;
4. while the NaOH solution concentration was 10 and 20 M, the compressive strength reached 21 MPa; and
5. as the amount of graphite in of graphite/calcite alkali active mortar increased, the compressive strength of the sample decreased; while the amount of calcite increased, the compressive strength of the sample increased.

Calcite and graphite are both considered to be suitable raw materials for alkali active mortar synthesis because they are cheap and abundant materials and provide good compressive strength.

Author contribution NK: Formation of the idea, experimental design, construction of experiments, evaluation of data, article writing and editing. SÇG: Formation of the idea, experimental design, evaluation of the data, editing of the article.

Funding This work was supported by the Cumhuriyet University Scientific Research Projects Unit (CUBAP) as Project Number M676.

Declarations

Conflict of interest The authors declare no competing interests.

References

1. Firdous, R., Hirsch, T., Klimm, D., Lothenbach, B., Stephan, D.: Reaction of calcium carbonate minerals in sodium silicate solution and its role in alkali-activated systems. *Miner. Eng.* **165**, 106849 (2021)
2. Zhang, B., Zhu, H., Feng, P., Zhang, P.: A review on shrinkage-reducing methods and mechanisms of alkali-activated/geopolymer systems: effects of chemical additives. *J. Build. Eng.* **49**(December 2021), 104056 (2022)
3. Kusak, I., Lunak, M., Rovnanik, P.: Electric conductivity changes in geopolymer samples with added carbon nanotubes. *Procedia Eng.* **151**, 157–161 (2016)
4. Al-saadi, T.H.A., Mohammad, S.H., Daway, E.G., Mejbel, M.K.: Synthesis of intumescent materials by alkali activation of glass waste using intercalated graphite additions. *Mater. Today Proc.* **42**, 1889–1900 (2021)
5. Prabaha, J., Vafaei, B., Baffoe, E., Ghahremaninezhad, A.: The effect of biochar on the properties of alkali-activated slag pastes. *Constr. Mater.* **2**(1), 1–14 (2021)
6. Gökçe, H.S., Tuyan, M., Nehdi, M.L.: Alkali-activated and geopolymer materials developed using innovative manufacturing techniques: a critical review. *Constr. Build. Mater.* **303**, 124483 (2021)
7. Zhang, Y., He, P., Yuan, J., Yang, C., Jia, D., Zhou, Y.: Effects of graphite on the mechanical and microwave absorption properties of geopolymer based composites. *Ceram. Int.* **43**(2), 2325–2332 (2017)
8. Murmu, A.L., Jain, A., Patel, A.: Mechanical properties of alkali activated fly ash geopolymer stabilized expansive clay. *KSCE J. Civ. Eng.* **23**(9), 3875–3888 (2019)
9. Meng, Y., Lei, J., Zhang, R., Yang, X., Zhao, Q., Liao, Y., et al.: Effect of geopolymer as an additive on the mechanical performance of asphalt. *Road Mater. Pavement Des.* **23**(11), 2466–2485 (2022)
10. Atabey, İİ: Influence of Ca and Al source on elevated temperature behavior of waste ceramic sanitaryware-based alkali-activated mortars. *J. Aust. Ceram. Soc.* **58**(3), 949–962 (2022)
11. Prabha, V.C., Revathi, V.: Geopolymer mortar incorporating high calcium fly ash and silica fume. *Arch. Civ. Eng.* **65**(1), 3–16 (2019)
12. Cheng, T.W., Lee, M.L., Ko, M.S., Ueng, T.H., Yang, S.F.: The heavy metal adsorption characteristics on metakaolin-based geopolymer. *Appl. Clay Sci.* **56**, 90–96 (2012)
13. Kütük, N., Çetinkaya, S.: Effect of kaolinite mass ratio on compressive strength of kaolinite-calcite based geopolymer. *IICESEN.* **3**(1), 25–28 (2017)
14. Yadollahi, M.M., Benli, A., Demirboğa, R.: Effects of elevated temperature on pumice based geopolymer composites. *Plast. Rubber Compos.* **44**, 226–237 (2015)
15. Deventer, J.S.J.V., Provis, J.L., Duxson, P.: Technical and commercial progress in the adoption of geopolymer cement. *Miner. Eng.* **29**, 89–104 (2012)
16. Temuujin, J., Riessen, A.V., Mackenzie, K.J.D.: Preparation and characterisation of fly ash based geopolymer mortars. *Constr. Build Mater.* **24**(10), 1906–1910 (2010)
17. Hamidi, R.M., Man, Z., Azizli, K.A.: Concentration of NaOH and the effect on the properties of fly ash based geopolymer. *Procedia Eng.* **148**, 189–193 (2016)
18. Erfanimesh, A., Sharbatdar, M.K.: Mechanical and microstructural characteristics of geopolymer paste, mortar, and concrete containing local zeolite and slag activated by sodium carbonate. *J. Build Eng.* **32**(May), 101781 (2020)
19. Liu, X., Jiang, B., Liao, G., Zuo, J., Xu, J., Shah, S.P.: Research on the smart behavior of MCNT grafted CF / cement-based composites. *Fuller. Nanotub. Carbon Nanostruct.* **29**(10), 844–851 (2021)
20. Cai, J., Wang, M., Zhou, S., Cheng, X.: Mechanical properties of graphite-oil well cement composites under high temperature. *ACS Omega.* **7**, 14148–14159 (2022)
21. Gebreegziabher, G.G., Asemahegne, A.S., Ayele, D.W., Dhakshnamoorthy, M.: One-step synthesis and characterization of reduced graphene oxide using chemical exfoliation method. *Mater. Today Chem.* **12**, 233–239 (2019)
22. Yip, C.K., Provis, J.L., Lukey, G.C., van Deventer, J.S.J.: Carbonate mineral addition to metakaolin-based geopolymers. *Cem. Concr. Compos.* **30**(10), 979–985 (2008)
23. Shahwan, T., Zünbül, B., Tunuso, Ö., Ero, A.E.: AAS, XRPD, SEM / EDS, and FTIR characterization of Zn²⁺ retention by calcite, calcite – kaolinite, and calcite – clinoptilolite minerals. *J. Colloid Interface Sci.* **286**, 471–478 (2005)
24. Gunasekaran, S., Anbalagan, G., Pandi, S.: Raman and infrared spectra of carbonates of calcite structure. *J. Raman Spectrosc.* **37**, 892–899 (2006)
25. Sauffi, A.S., Mastura, W., Ibrahim, W., Mustafa, M., Bakri, A., Ahmad, R., et al.: A review of carbonate minerals as an additive to geopolymer materials a review of carbonate minerals as an additive to geopolymer materials. *IOP Conf. Ser. Mater. Sci. Eng.* **551**, 012084 (2019)
26. Aboulayt, A., Gounni, A., El Alami, M., Hakkou, R., Hannache, H., Gomina, M., et al.: Thermo-physical characterization of a metakaolin-based geopolymer incorporating calcium carbonate: a case study. *Mater. Chem. Phys.* **252**(March), 123266 (2020)

27. Abdel-Gawwad, H.A., Rashad, A.M., Heikal, M.: Sustainable utilization of pretreated concrete waste in the production of one-part alkali-activated cement. *J.Clean Prod.* **232**, 318–328 (2019)
28. Degirmenci, F.N.: Effect of sodium silicate to sodium hydroxide ratios on durability of geopolymer mortars containing natural and artificial pozzolan. *Ceram. Silik.* **61**(4), 340–350 (2017)
29. Al Bakri, M., Kamarudin, H., Bnhussain, M., Khairul Nizar, I., Rafiza, A.R., Izzat, A.M.: Chemical reactions in the geopolymerisation process using fly ash-based geopolymer: a review 1. *Aust. J. Basic Appl. Sci.* **5**(7), 1199–1203 (2011)
30. El-Mahllawy, M.S., Kandeel, A.M., Abdel Latif, M.L., El Nagar, A.M.: The feasibility of using marble cutting waste in a sustainable building clay industry. *Recycling.* **3**(3), 39 (2018)
31. Saraya, M.E.-S.I., Rokbaa, H.H.A.L.: Preparation of vaterite calcium carbonate in the form of spherical nano-size particles with the aid of polycarboxylate superplasticizer as a capping agent. *Am. J. Nanomater.* **4**(2), 44–51 (2016)
32. Al-saadi, T.H.A., Daway, E.G., Mohammad, S.H.: Effect of graphite additions on the intumescent behaviour of alkali-activated materials based on glass waste. *J. Mater. Res. Technol.* **9**(6), 14338–14349 (2020)
33. Aliyeva, S., Aliyev, E., Maharramov, A., Alosmanov, R., Buniyatzadeh, I., Eyvazova, G., et al.: Synthesis of o-phenylenediamine functionalized graphite. *Fuller. Nanotub. Carbon Nanostruct.* **25**(5), 306–311 (2017)
34. Siburian, R., Sari, D.R., Gultom, J., Sihotang, H., Raja, S.L., Gultom, J., et al.: Performance of graphite and graphene as electrodes in primary cell battery. *J. Phys. Conf. Ser.* **1116**(4), 042034 (2018)
35. Baykara, H., Cornejo, M.H., García, E., Ulloa, N.: Preparation, characterization, and evaluation of compressive strength of polypropylene fiber reinforced geopolymer mortars. *Heliyon.* **6**(4), e03755 (2020)
36. Tanpure, S., Ghanwat, V., Shinde, B., Tanpure, K., Lawande, S.: The eggshell waste transformed green and efficient synthesis of K-Ca (OH)₂ catalyst for room temperature synthesis of chalcones. *Polycycl. Aromat. Compd.* **42**(4), 1322–1340 (2022)
37. Fiocco, L., Michielsen, B., Bernardo, E.: Silica-bonded apatite scaffolds from calcite-filled preceramic polymers. *J. Eur. Ceram. Soc.* **36**(13), 3211–3218 (2016)
38. Cai, G.B., Chen, S.F., Liu, L., Jiang, J., Yao, H.B., Xu, A.W., et al.: 1,3-Diamino-2-hydroxypropane-N, N, N', N'-tetraacetic acid stabilized amorphous calcium carbonate: nucleation, transformation and crystal growth. *CrystEngComm.* **12**(1), 234–241 (2010)
39. Wang, X., Yang, W., Liu, H., Zhu, P., Zong, N., Feng, J.: Strength and microstructural analysis of geopolymer prepared with recycled geopolymer powder. *J. Wuhan Univ. Technol. Mater Sci. Ed.* **36**(3), 439–445 (2021)
40. Payakaniti, P., Chuewangkam, N., Yensano, R., Pinitsoontorn, S., Chindaprasirt, P.: Changes in compressive strength, microstructure and magnetic properties of a high-calcium fly ash geopolymer subjected to high temperatures. *Constr. Build Mater.* **265**, 120650 (2020)
41. Liang, Z., Wang, Q., Dong, B., Jiang, B., Xing, F.: Ion-triggered calcium hydroxide microcapsules for enhanced corrosion resistance of steel bars. *RSC Adv.* **8**(39536), 39536–39544 (2018)
42. Samimi, K., Pakan, M., Eslami, J.: Investigating the compressive strength and microstructural analysis of mortar containing synthesized graphene and natural pozzolan in the face of alkali-silica reactions. *J. Build Eng.* **68**(February), 106126 (2023)
43. Tchadjjié, L.N., Djobo, J.N.Y., Ranjbar, N., Tchakouté, H.K., Kenne, B.B.D., Elimbi, A.: Potential of using granite waste as raw material for geopolymer synthesis. *Ceram. Int.* **42**(2), 3046–3055 (2016)
44. Qin, Y., Yu, L., Wu, R., Yang, D., Qiu, X., Zhu, J.Y.: Biorefinery lignosulfonates from sulfite-pretreated softwoods as dispersant for graphite. *ACS Sustain. Chem. Eng.* **4**(4), 2200–2205 (2016)
45. Polat, S., Demiray, B., Tekin, B., Kardaş, M.: An investigation of polymorphism of calcium carbonate in the presence of proline. *AKU J. Sci. Eng.* **20**, 883–891 (2020)
46. Lv, Q., Yu, J., Ji, F., Gu, L., Chen, Y., Shan, X.: Mechanical property and microstructure of fly ash-based geopolymer activated by sodium silicate. *KSCE J. Civ. Eng.* **25**(5), 1765–1777 (2021)
47. Ouyang, S., Chen, W., Zhang, Z., Li, X.: Experimental study of one-part geopolymer using different alkali sources. *J. Phys. Conf. Ser.* **1606**, 012155 (2020)
48. Abdullah, A., Hussin, K., Abdullah, M.M.A.B., Yahya, Z., Sochacki, W., Razak, R.A., et al.: The effects of various concentrations of NaOH on the inter-particle gelation of a fly ash geopolymer aggregate. *Materials (Basel).* **14**(5), 1–11 (2021)
49. Tippayasam, C., Sutikulsoombat, S., Kamseu, E., Rosa, R., Thavorniti, P., Chindaprasirt, P., et al.: In vitro surface reaction in SBF of a non-crystalline aluminosilicate (geopolymer) material. *J. Aust. Ceram. Soc.* **55**(1), 11–17 (2019)
50. Aboulayt, A., Riahi, M., Ouazzani Touhami, M., Hannache, H., Gomina, M., Moussa, R.: Properties of metakaolin based geopolymer incorporating calcium carbonate. *Adv. Powder Technol.* **28**(9), 2393–2401 (2017)
51. Bayiha, B.N., Billong, N., Yamb, E., Kaze, R.C., Nzengwa, R.: Effect of limestone dosages on some properties of geopolymer from thermally activated halloysite. *Constr. Build Mater.* **217**, 28–35 (2019)
52. Bakkali, H., Ammari, M., Frar, I.: NaOH alkali-activated class F fly ash: NaOH molarity, Curing conditions and mass ratio effect. *J. Mater. Environ. Sci.* **7**(2), 397–401 (2016)
53. Kamarudin, H., Bakri, A.M.M.A., Binhussain, M., Ruzaidi, C.M., Luqman, M., Heah, C.Y.: Preliminary study on effect of NaOH concentration on early age compressive strength of kaolin-based green cement. *Int. Conf. Chem. Chem. Process.* **10**, 18–24 (2011)
54. Ng, H.T., Heah, C.Y., Liew, Y.M., Abdullah, M.M.A.B.: The effect of various molarities of NaOH solution on fly ash geopolymer paste. *AIP Conf. Proc.* **2045**(December), 10–15 (2018)
55. Kalinkin, A., Chislov, M.V., Kalinkina, E.V., Zvereva, I.A., Cherkezova-zheleva, Z., Paneva, D., et al.: Synthesis of Fly ash-based geopolymers: effect of calcite addition and mechanical activation. *Minerals.* **10**(9), 827 (2020)
56. Mizerová, C., Kusák, I., Rovnaník, P.: Electrical properties of fly ash geopolymer composites with graphite conductive admixtures. *Acta Polytech. CTU Proc.* **22**, 72–76 (2019)
57. Rovnaník, P., Šimonová, H., Topolář, L., Keršner, Z.: Mechanical fracture properties of alkali-activated slag with graphite filler. *Procedia Eng.* **190**, 43–48 (2017)
58. Yetgin, S.H., Çolak, M.: Investigation of mechanical and tribological properties of graphite filled polypropylene composites. *El-Cezeri J. Sci. Eng.* **7**(2), 649–658 (2020)
59. Arioz, E., Arioz, O., Kockar, O.M.: Geopolymer synthesis with low sodium hydroxide concentration. *Iran J. Sci. Technol. Trans. Civ. Eng.* **44**(s1), 525–533 (2020)
60. Mikhailova, O., Rovnaník, P.: Effect of polyethylene glycol addition on metakaolin-based geopolymer. *Procedia Eng.* **151**, 222–228 (2016)
61. Rakhimova, N.R., Rakhimov, R.Z., Naumkina, N.I., Khuzin, A.F., Osin, Y.N.: Influence of limestone content, fineness, and composition on the properties and microstructure of alkali-activated slag cement. *Cem. Concr. Compos.* **72**, 268–274 (2016)

Publisher's note Springer Nature remains neutral with regard to jurisdictional claims in published maps and institutional affiliations.

Springer Nature or its licensor (e.g. a society or other partner) holds exclusive rights to this article under a publishing agreement with the author(s) or other rightsholder(s); author self-archiving of the accepted manuscript version of this article is solely governed by the terms of such publishing agreement and applicable law.